Vol. 690: 51–64, 2022
https://doi.org/10.3354/meps14042

MARINE ECOLOGY PROGRESS SERIES
Mar Ecol Prog Ser

Published June 2

Variability in antimicrobial chemical defenses in the Caribbean sponge *Agelas tubulata*: implications for disease resistance and resilience

Amelia Clayshulte Abraham[1], Deborah J. Gochfeld[1,2], Bharathi Avula[2], Keir J. Macartney[3], Michael P. Lesser[3], Marc Slattery[1,4,*]

[1]Department of Biomolecular Sciences, Division of Environmental Toxicology, University of Mississippi, University, MS 38677, USA

[2]National Center for Natural Products Research, University of Mississippi, University, MS 38677, USA

[3]Department of Molecular, Cellular and Biomedical Sciences and School of Marine Science and Ocean Engineering, University of New Hampshire, Durham, NH 03824, USA

[4]Department of Biomolecular Sciences, Division of Pharmacognosy, University of Mississippi, University, MS 38677, USA

ABSTRACT: Sponges in the genus *Agelas* produce a diversity of bromopyrrole alkaloid secondary metabolites, some of which are known to inhibit predators and pathogens. Selective pressures on sponges to produce chemical defenses vary in time and space, often resulting in differences in the production of secondary metabolites. To characterize intraspecific variation in these compounds, we generated metabolomic profiles of the Caribbean sponge *A. tubulata* across spatial gradients, including multiple sites in Belize and Grand Cayman, and depths ranging from 15 to 61 m in Grand Cayman. Samples were also analyzed from a reciprocal transplant experiment across shallow (22 m) to mesophotic (61 m) reefs. We found quantitative, but not qualitative, differences in metabolite profiles across sites and depths, with 9 metabolites contributing to that variation. In addition, transplanting sponges across depths resulted in significant changes in concentrations of the metabolite sceptrin. Sponge extracts exhibited antibacterial activity against a panel of marine and human pathogens. Multiple regression analyses showed that different metabolites were associated with antibacterial activity against different pathogens. The strongest compound-specific relationship was a negative effect of oroidin on the growth of *Serratia marcescens,* and purified oroidin was found to inhibit *S. marcescens* growth in a dose-dependent manner. Overall, *A. tubulata* exhibits intraspecific variability in the production of antibacterial secondary metabolites across sites and depths that signals selective responses to its environment. Given the current increase in sponge densities, and incidence of disease on coral reefs, these data have implications for disease resistance and resilience of sponges in the Anthropocene.

KEY WORDS: *Agelas tubulata* · Antibacterial chemical defense · Biogeographic variability · Bromopyrrole alkaloids · Caribbean · Mesophotic coral ecosystem · Sponge

1. INTRODUCTION

Sponges represent one of the most diverse taxa on Caribbean coral reefs (Van Soest et al. 2012), have been reported to be increasing in density (Bell et al. 2013), and produce a diversity of secondary metabolites that play important ecological roles (Pawlik 2011, Han et al. 2019, Wulff 2021). Due to their sessile lifestyle, many sponges rely on secondary metabolites for defense against predation (Pawlik 2012), competition (Slattery & Gochfeld 2012), microbial overgrowth (Newbold et al. 1999, Kelly et al. 2005,

*Corresponding author: slattery@olemiss.edu

Qian & Xu 2012), and/or pathogenesis (Gochfeld et al. 2012, Slattery & Gochfeld 2012). Optimal defense theory predicts that the biosynthesis of defensive metabolites could come at the expense of energy invested in primary physiological functions, such as growth and reproduction (Cronin 2001). Thus, it would be advantageous for individual sponges to produce these defenses in response to ephemeral ecological threats, such as predation or disease outbreaks (Karban & Baldwin 1997). As these threats also vary across spatial gradients (e.g. predation: Loh et al. 2014; pathogenesis: Easson et al. 2013), it is predicted that the concentrations of defensive metabolites will vary throughout a metapopulation. Intraspecific variation in defensive chemistry has been documented in several sponge taxa across their biogeographic and depth ranges (e.g. Thompson et al. 1987, Sacristán-Soriano et al. 2011, Rohde et al. 2012, Slattery et al. 2016, Reverter et al. 2016, 2018, Bayona et al. 2020).

Regulation of chemical phenotypes is predicted to occur at 1 of 2 levels. If ecological pressures remain relatively stable through time, then production of defensive metabolites is also predicted to remain stable (i.e. constitutive; Slattery et al. 2001). Alternatively, if the ecological pressures that select for defensive metabolites vary over time and/or space, then production of certain defensive metabolites may also vary (i.e. inducible; Pavia & Toth 2000, Slattery et al. 2016), with their dynamic regulation occurring at the level of gene expression (Strauss & Reyes-Dominguez 2011).

Sponges of the genus *Agelas* are common constituents of Caribbean reefs and represent a rich source of secondary metabolites (i.e. halogenated alkaloids: Rane et al. 2014, Zhang et al. 2017) that exhibit antipredator, antimicrobial, antifouling, and allelopathic bioactivities (e.g. Chanas et al. 1997, Assmann et al. 2004). Intraspecific variation in gross biochemical composition across broad geographic scales has also been observed in at least one species, *A. tubulata* (Clayshulte Abraham et al. 2021). This variation in primary metabolism is likely due to differential ecological pressures across the Caribbean basin (e.g. predation: Loh & Pawlik 2014), which may also impact secondary metabolism in conspecific sponges collected from different sites. Likewise, an increase in bacterioplankton with depth (Lesser 2006, Lesser & Slattery 2013) might select for increased production of antimicrobial compounds to regulate bacterial communities and inhibit pathogenesis (Taylor et al. 2007, Slattery & Gochfeld 2012, Raina et al. 2016). By surveying individual *A. tubulata* secondary metabolite profiles and antimicrobial bioactivity across a geographic and depth gradient, the following hypotheses were addressed: (1) the production of *A. tubulata* secondary metabolites will vary between sites and depths, (2) sponge secondary metabolite profiles will exhibit phenotypic plasticity when transplanted between depths, and (3) variability in secondary metabolite production will translate into differences in antibacterial bioactivity between sponge populations.

2. MATERIALS AND METHODS

2.1. Sample collection

Samples of *Agelas tubulata* were collected from 3 sites in Belize (Carrie Bow Cay: 16° 48.005′ N, 88° 04.668′ W; Curlew Cay: 16° 47.350′ N, 88° 04.571′ W; Southwater Cay: 16° 48.986′ N, 88° 04.629′ W) in June 2017, and from 3 sites in Grand Cayman (Kittiwake Anchor Chain: 19° 21.718′ N, 81° 24.138′ W; Sentinel Rock: 19° 22.075′ N, 81° 24.990′ W; Slaughterhouse Wall: 19° 21.776′ N, 81° 24.250′ W) in January 2018. Sponge samples (n = 5–10 per site) were collected from a depth of 15 m on typical Caribbean spur-and-groove buttresses. At Kittiwake Anchor Chain, additional samples were collected at 22, 30, 46, and 61 m (n = 5 per depth). Samples were cut from individual sponges at each site and depth, placed in numbered resealable plastic bags, and returned to shore facilities where they were stored at −20°C for 1–2 wk prior to transport and processing at the University of Mississippi.

2.2. Transplant experiment

In addition to the collections of *A. tubulata* across sites and depths described above, samples from a transplant experiment were analyzed to determine whether the sponge secondary metabolites exhibited phenotypic plasticity when transplanted between depths. Briefly, at Kittiwake Anchor Chain, replicate sponges (n = 20) were transplanted between 22 and 61 m in a fully orthogonal (i.e. with transplant controls) genotype-controlled reciprocal experiment, as described by Macartney et al. (2021). Specifically, sponge ramets were transplanted into numbered PVC racks at each depth, with treatments (n = 5 genets per treatment) consisting of ramets from deep (61 m) sponges transplanted to the shallow depth (22 m, treatment ‘D-S’) and ramets from the same

sponges back-transplanted to their site of origin (i.e. deep to deep handling controls, D-D). Similarly, ramets of shallow (22 m) sponges were transplanted to the deep depth (61 m, S-D), and back-transplanted to their site of origin (i.e. shallow to shallow handling controls, S-S). The transplant experiment ran for 18 mo during 2018 and 2019 (Macartney et al. 2021), and sponges were then collected for multiple analyses. As described by Clayshulte Abraham et al. (2021), sample wet mass, volume, and dry mass were quantified prior to chemical analyses. Approximately 300 mg of ground freeze-dried sponge tissue were extracted 3 times in 10 ml of 1:1 methanol:methylene chloride (MeOH:DCM) in a sonicator. The solvent was removed via vacuum centrifugation, and the dried extract mass was recorded. Extract dry mass was then converted into a volumetric concentration based on sample mass:volume relationships (e.g. Gochfeld et al. 2012) for subsequent antibacterial assays (see Section 2.4).

2.3. Metabolomic profiling of sponge compounds

A. tubulata extracts were dissolved in MeOH at a concentration of 5 mg ml^{-1}, and 20 µl were injected into a Waters Alliance 2695 high performance liquid chromatography (HPLC) system, coupled to a Waters 2996 photodiode array detector. Individual compounds were separated across a Phenomenex Gemini C18 column (4.6 × 250 mm, 5 µm) using a gradient solvent system comprised of HPLC grade water (H_2O) and acetonitrile (ACN), both containing 0.1% trifluoracetic acid. Starting run conditions were 90% H_2O:10% ACN, and ramped up to 45% H_2O:55% ACN over the course of 30 min at a flow rate of 1 ml min^{-1}. Peak absorbances were measured at 254 nm, and peak areas for 11 peaks were integrated using the Waters Empower2 software. For each peak, the area under the curve was used in statistical analyses to compare relative concentrations of individual peaks among extracts (Gochfeld et al. 2012).

Representative extracts of *A. tubulata* from 15 m (n = 3) were selected for analysis by liquid chromatography coupled with mass spectrometry (LC-MS) based on the presence, and clear distinction, of the greatest number of peaks. Extracts were dissolved in MeOH to 5 mg ml^{-1} and separated by HPLC (Agilent Series 1290 system) across an Agilent Poroshell 120 EC C-18 column (2.1 × 150 mm, 2.7 µm) using a gradient solvent system comprised of HPLC grade H_2O and ACN, both containing 0.1% formic acid. Starting run conditions were 99% H_2O:1% ACN and these were ramped to 55% H_2O:45% ACN over the course of 30 min at a flow rate of 0.2 ml min^{-1}. Peak absorbances were measured at 254 nm, at a column temperature of 35°C. A mass spectrometric analysis was performed with quadrupole time of flight tandem mass spectrometry (Agilent g6530A QToF-MS/MS). All operations, acquisition, and analysis of data were controlled by the Agilent MassHunter Acquisition software (version A.05.00) and processed with MassHunter Qualitative Analysis software (version B.07.00). Each sample was analyzed in both positive and negative modes in the range of m/z = 100–2500. Accurate mass measurements were obtained by means of ion correction techniques, and the compounds were confirmed in each spectrum. The identities of oroidin and sceptrin were confirmed using a standard practice of comparison to purified standards (e.g. Rohde et al. 2012). However, standards were not available for the remaining 9 compounds, so the mass spectra were compared to the molecular masses of compounds reported to occur within the genus *Agelas*, using the online databases MarinLit (version 2021.0.4.0), SciFinder (version 2021), and the Dictionary of Natural Products (version 29.2.2020). These data must be considered with some caution since this approach might not distinguish between related isomers with the same molecular mass (e.g. peak 8, see Section 3.1).

2.4. Antibacterial assays

Although *A. tubulata* is susceptible to disease (Deignan & Pawlik 2016, D. Gochfeld unpubl. data), putative pathogen(s) affecting this species have been neither identified nor isolated to date (Deignan et al. 2018). Thus, *A. tubulata* extracts were screened against a panel of bacterial pathogens associated with coral diseases and/or poor water quality that might also impact marine sponge health (Gochfeld & Aeby 2008, Gochfeld et al. 2012, Rohde et al. 2012). These bacteria included the coral pathogens *Aurantimonas coralicida* (Denner et al. 2003), *Serratia marcescens* (Patterson et al. 2002), and *Vibrio coralliilyticus* (Ben-Haim et al. 2003), as well as *Yersinia enterocolitica*, a common human enteric pathogen that has been found in sewage runoff in coastal marine waters (Kilinc & Besler 2014).

Bacteria were cultured following specifications by the American Type Culture Collection (ATCC, Manassas, VA, USA) and the Deutsche Sammlung von Mikroorganismen und Zellkulturen (DSMZ, Braunschweig, Germany). Briefly, all bacteria were cul-

tured in a rocking incubator; *A. coralicida* and *V. coralliilyticus* in marine broth at their optimal growth temperature of 28°C, *S. marcescens* in trypticase soy broth at 28°C, and *Y. enterocolitica* in tryptose broth at 37°C. Bacteria were inoculated into 10 ml of their respective media and allowed to grow overnight, the optical densities at 600 nm (OD_{600}) were measured on an Eppendorf Biophotometer, and the cultures were diluted with media to an OD_{600} of 0.1. Sponge extracts (n = 76) were diluted to a stock concentration of 100 mg ml^{-1} in dimethyl sulfoxide (DMSO), and 10 µl of crude sponge extract were added to 190 µl of the bacterial cultures, for a final test concentration of 5 mg ml^{-1}. This represented 2.5–10% of the natural extract concentrations. The total concentration of DMSO by volume was maintained at 5% in order to prevent cytotoxicity from the solvent itself (de Brito et al. 2017), and concentrations of DMSO from 0.25 to 5.5% were confirmed not to inhibit growth of the test bacteria (M. Ansley & D. Gochfeld unpubl. data). Extract-treated bacterial cultures were pipetted into 96-well plates, and the initial OD_{600} (T_0) was recorded using a BioTek Synergy HT Multi-Detection Microplate Reader. Plated cultures were allowed to grow for 24 h at their culture temperatures, and the OD_{600} was recorded again (T_{24}). On each plate, controls for the extract-treated cultures included 200 µl of the bacterial culture alone (negative control), and antibiotic-treated bacterial cultures (195 µl of bacterial culture and 5 µl of 1 mg ml^{-1} ciprofloxacin, a broad-spectrum antibiotic as a positive control). In addition, wells containing media alone were used to confirm sterility of culture conditions. To normalize for background absorbance of the extracts themselves, we subtracted the OD_{600} at T_0 from the OD_{600} at T_{24} h for each well (e.g. Wang et al. 2010); we previously determined that the OD_{600} of extracts dissolved in media did not change significantly during the 24 h incubation period. All extracts and controls were run in triplicate, with the 3 wells for each treatment representing procedural controls that were later averaged for each biological replicate (Gochfeld & Aeby 2008). We used the ratio of bacterial growth in treated vs. untreated wells over a 24 h period to measure inhibitory or growth-promoting activities of extracts. Ratios <1 indicated antibacterial activity, ratios >1 indicated growth-promoting activity, and ratios of 1 indicated no activity in the assay. A dose response experiment utilizing *S. marcescens* was performed in a similar manner but with select sponge extracts representing low, intermediate, and high concentrations of oroidin, along with purified oroidin (the only pure metabolite available for this analysis), serially diluted in DMSO. Sigmoidal dose response curves were fitted, and EC_{25} values were calculated using SigmaPlot 14.0.

2.5. Statistics

Differences in the metabolomic profiles between sponges collected from 15 m depth across sites (i.e. 3 sites in Belize and 3 sites in Grand Cayman), different depths (Grand Cayman), and transplants within and between depths (Grand Cayman), were assessed by comparing areas under the curve for HPLC peaks 1–11 (Fig. 1) with 1-way permutational multivariate analyses of variance (PERMANOVAs) using the 'adonis2' function in the R package 'vegan' (version 2.5-7; Oksanen et al. 2020). For each of the predictor variables of site, depth, or transplant treatment, separate 1-way ANOVAs were also conducted on the individual peaks, to identify differences among specific chemical constituents. Normality of each response variable was assessed by plotting histograms of the residuals, and homoscedasticity of the response variables was assessed by graphing the residuals against the predicted values (Kozak & Piepho 2018).

Antibacterial activity of sponge extracts from different sites, depths, and transplant treatments was assessed by comparing the ratio of bacterial growth in treated vs. untreated wells using a Student's 2-tailed *t*-test, with a null hypothesis that the ratio equals 1 if extracts exhibit no antibacterial activity. Differences in antibacterial activity against the 4 bacterial species were analyzed using 1-way ANOVAs based on the predictor variables of site, depth, or transplant treatment. Within each analysis, pairwise comparisons between sites, depths, and transplant treatments were conducted using Tukey's honestly significant difference post hoc tests, with p-values Bonferroni corrected for multiple testing. To determine which compounds were most likely responsible for antibacterial activity, multiple regression analysis was conducted using individual HPLC peak areas for all 11 peaks as the predictor variables, and the ratio of treated to untreated bacterial growth as the response variable. The magnitude of the antibacterial effects of the extracts were tested using Cohen's f^2 effects sizes. Final models with the lowest corrected Akaike's information criterion (AIC_c) scores were selected. Cook's distances were calculated and did not identify any outliers that were overly influencing the model. Plots were generated with the R packages 'dplyr,' 'ggplot2,' and 'gridExtra.' All statistical analyses were conducted in R version 4.0.2 (R Core Team 2020).

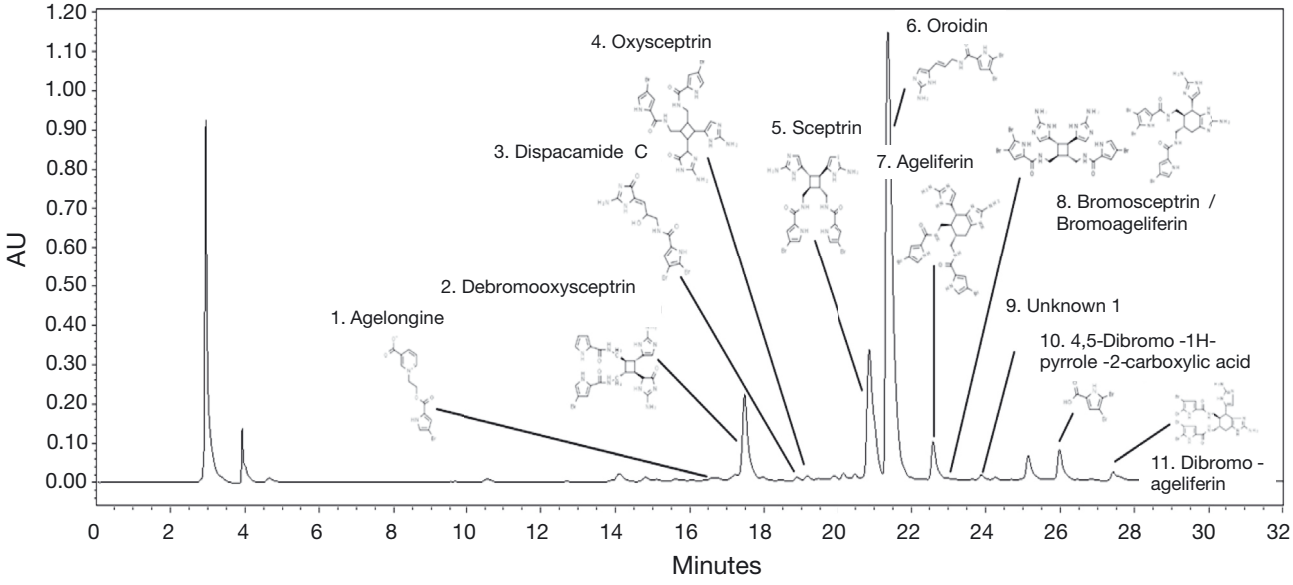

Fig. 1. Representative HPLC chromatogram of metabolites in *Agelas tubulata* extracts. Absorbance units (AU) at 254 nm shown on the *y*-axis and retention time (min) for individual peaks on the *x*-axis. Structures of most likely compound identities were determined by liquid chromatography-mass spectrometry and compared to published molecular masses (MM) of known *Agelas* compounds. Compound names and structures are denoted above peaks. The MM for peak 8 corresponds to that of both bromosceptrin and bromoageliferin; thus, its likely identity could not be differentiated, and it is referred to as bromosceptrin/bromoageliferin. The MM of peak 9 could not be confirmed and is referred to as 'Unknown 1'

3. RESULTS

3.1. Composition of *Agelas tubulata* extracts

For the analysis of *A. tubulata* extract constituents, we quantified 11 distinct peaks representing secondary metabolites. The most likely compound identities for 9 of the peaks were assigned based on published molecular masses of compounds identified from the genus *Agelas* (Fig. 1; Table S1 in the Supplement at www.int-res.com/articles/suppl/m690p051_supp.pdf). All identified compounds were either bromopyrrole alkaloids (peaks 1–8 and 11), or their derivatives (peak 10) (Fig. 1). Peak 9 ('unknown 1'; Fig. 1) was not identifiable because we could not obtain a molecular mass, but it was quantified for comparison among sponges. The molecular mass of peak 8 was consistent with that of both bromosceptrin and bromoageliferin (Fig. 1; Table S1), which could not be differentiated in this analysis, so this peak is referred to as bromosceptrin/bromoageliferin.

3.2. Spatial variation in the concentration and composition of *A. tubulata* extracts

The total tissue extract concentration for *A. tubulata* did not vary significantly across sites at 15 m (1-way ANOVA: df = 5, $F = 1.68$, p = 0.17; Fig. S1A). However, extract concentration increased with increasing depth in Grand Cayman, with significant differences between 15 and 61 m (65.4 ± 6.6 and 181.9 ± 35.8 mg ml^{-1} of sponge tissue, respectively [mean ± SE]; 1-way ANOVA: df = 4, $F = 8.55$, $p < 0.0001$; Fig. S1B).

Overall, extract composition varied significantly both by site and across the depth gradient (PERMANOVA: $F \leq 3.2$; $p < 0.003$), but not between treatments in the reciprocal transplant experiment (PERMANOVA: $F = 2.5$; $p = 0.07$). Although we quantified 11 peaks, only 9 varied significantly across sites or depths (Table 1). Seven compounds varied by site, including agelongine, debromooxysceptrin, oxysceptrin, oroidin, ageliferin, unknown compound 1, and 4,5-dibromo-1H-pyrrole-2-carboxylic acid (Table 1, Fig. 2). Four compounds, including agelongine, dispacamide C, bromosceptrin/bromoageliferin, and unknown 1, varied across the depth gradient (Table 1, Fig. 3). One compound, sceptrin, varied significantly across treatment groups in the transplant experiment (Table 1). Specifically, sceptrin concentrations were significantly lower at the deep site (61 m) and higher at the shallow site (22 m), and deep to shallow (D-S) transplants approached the metabolite concentrations of resident conspecifics (i.e. the back-transplants [S-S]; Fig. 4, and see Fig. S2).

Table 1. Summary of 1-way ANOVAs comparing relative concentration of each compound in terms of peak area within *Agelas tubulata* extracts among collection sites (at 15 m), depths (15– 61 m), and transplant treatments (shallow to shallow, shallow to deep, deep to shallow, and deep to deep)

Peak ID	Compound	Site			Depth			Transplant		
		df	*F*	p	df	*F*	p	df	*F*	p
1	Agelongine	5,33	6.73	0.0002	4,34	10.52	<0.0001	3,13	0.41	0.7474
2	Debromooxysceptrin	5,33	12.92	<0.0001	4,34	1.15	0.3481	3,13	1.53	0.2533
3	Dispacamide C	5,33	1.74	0.1524	4,34	6.32	0.0006	3,13	0.29	0.8309
4	Oxysceptrin	5,33	6.11	0.0004	4,34	1.27	0.3008	3,13	2.18	0.1391
5	Sceptrin	5,33	0.58	0.7106	4,34	0.37	0.8300	3,13	3.58	0.0440
6	Oroidin	5,33	7.03	<0.0001	4,34	2.43	0.0684	3,13	2.10	0.1494
7	Ageliferin	5,33	12.34	<0.0001	4,34	0.67	0.6203	3,13	1.01	0.4108
8	Bromosceptrin/ Bromoageliferin	5,33	0.73	0.6065	4,34	11.51	<0.0001	3,13	0.75	0.5403
9	Unknown 1	5,33	4.20	0.0046	4,34	4.27	0.0066	3,13	1.40	0.2867
10	4,5-Dibromo-1H-pyrrole-2-carboxylic acid	5,33	4.66	0.0025	4,34	1.12	0.3647	3,13	0.72	0.5550
11	Dibromoageliferin	5,33	1.09	0.3852	4,34	2.00	0.1166	3,13	0.62	0.6225

3.3. Antibacterial activity of *A. tubulata* extracts

At the tested concentration (5 mg ml^{-1}), which represents 2.5–10% of natural concentrations, *A. tubulata* extracts from each site, depth, and transplant treatment significantly inhibited the growth of all bacterial species tested (Student's *t*-tests: $p \leq 0.05$; Table S2), except for *Yersinia enterocolitica* in the shallow to deep (S-D) transplant treatment (Student's *t*-test: $t = -3.97$, $p = 0.09$; Table S2). We also found significant differences in the degree of inhibitory activity against *Serratia marcescens* and *Vibrio coralliilyticus* across depths (ANOVA: df = 4, $F = 5.6$, $p < 0.002$ and $F = 4.1$, $p < 0.009$, respectively; Fig. 5), but not across sites or transplant treatments.

3.4. Putative compounds associated with antibacterial activity of *A. tubulata* extracts

To determine which compound(s) contributed to the antibacterial activity of the *A. tubulata* extracts, we conducted multiple regression analyses on the HPLC peak areas relative to the growth of extract-treated bacteria. We found that the relative concentration of dibromoageliferin was positively correlated with the growth of *S. marcescens* and *V. coralliilyticus* (Table 2). In contrast, 4,5-dibromo-1H-pyrrole-2-carboxylic acid was negatively correlated with the growth of *S. marcescens* and *V. coralliilyticus*. Agelongine was also negatively correlated with the growth of *V. coralliilyticus*, as well as *Y. enterocolitica*. Finally, oroidin was negatively correlated with the growth of *S. marcescens* (Table 2, Fig. 6). In contrast, the activities of debromooxysceptrin and oxysceptrin were species-specific. Debromooxysceptrin was negatively correlated with the growth of *S. marcescens*, but positively correlated with the growth of *Aurantimonas coralicida*, and oxysceptrin was negatively correlated with the growth of *S. marcescens* and *V. coralliilyticus*, but positively correlated with the growth of *Y. enterocolitica* (Table 2). Of all pairwise tests of bacterial-compound combinations, the largest effect size was the effect of oroidin on the growth of *S. marcescens* ($f^2 = 1.67$, $p < 0.0001$; Table 2, Fig. 6).

To confirm that oroidin is, at least in part, responsible for the inhibitory activity of *A. tubulata* extracts on *S. marcescens* growth, we performed a dose response experiment using purified oroidin and 3 representative *A. tubulata* extracts that contained low (KY-AGTU-200-2: peak area = 5 054 838), intermediate (BZ-AGTU-20: peak area = 16 128 295), and high (KY-AGTU-7: peak area = 32 252 527) relative concentrations of oroidin, as determined by HPLC. Consistent with our multiple regression model (Table 2, Fig. 6), we found that purified oroidin inhibited the growth of *S. marcescens* in a dose-dependent manner, with an EC_{25} of 0.48 mg ml^{-1} or 1.2 mM (Fig. 7). Additionally, the *A. tubulata* extract with the highest oroidin content had the lowest EC_{25} (0.13 mg ml^{-1}), whereas the extracts with the intermediate and lowest oroidin content had higher EC_{25} values (0.71 and 1.95 mg ml^{-1}, respectively; Fig. 7), which is consistent with the prediction that higher levels of oroidin resulted in increased antibacterial activity against *S. marcescens*. The EC_{25} of the *A. tubulata* extract with the highest

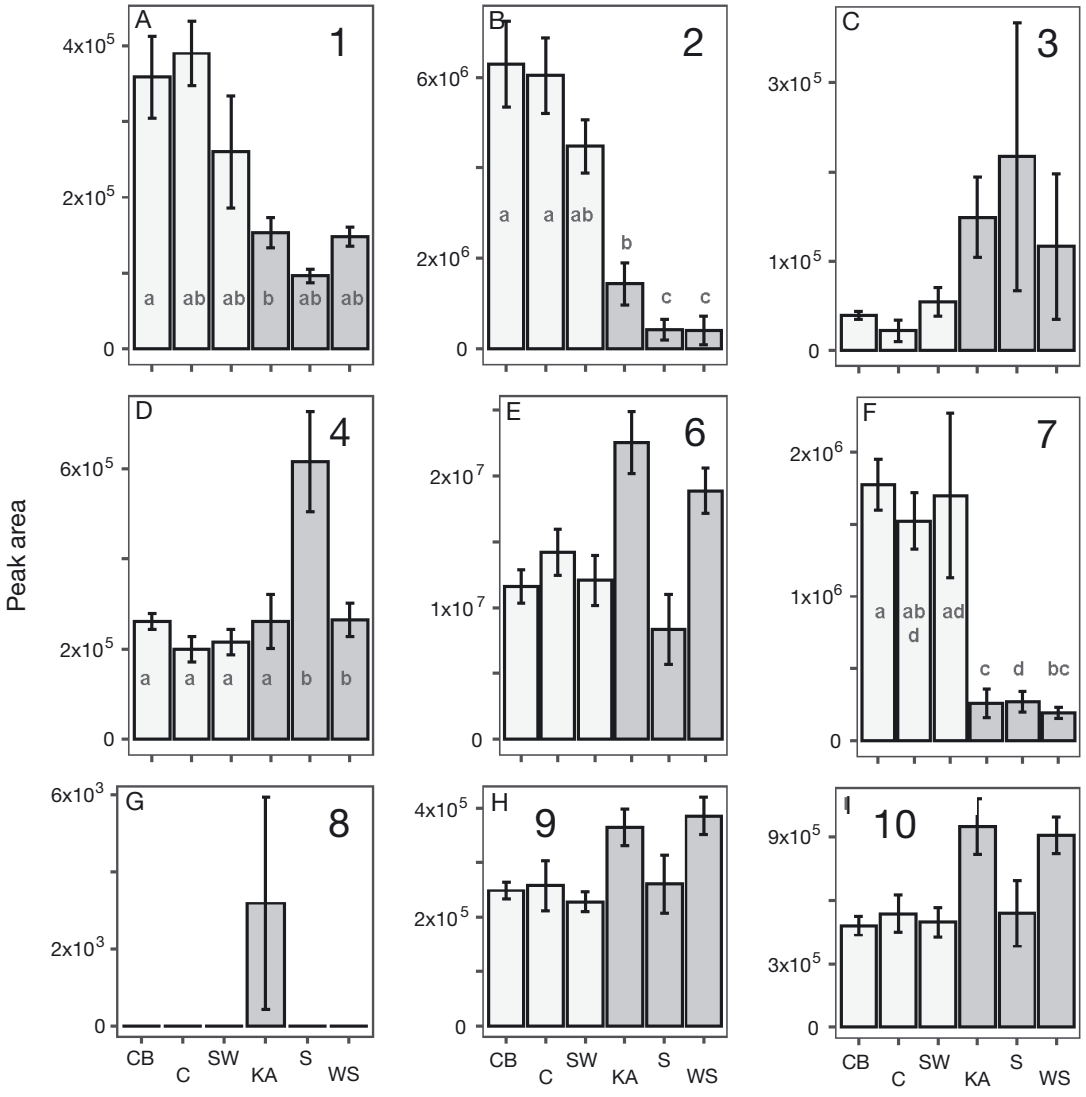

Fig. 2. Relative abundance of individual compounds within *Agelas tubulata* extracts by collection site. Bars represent the mean (±SE) peak area of individual compounds within extracts from sponges collected from 15 m at different sites in Belize (light bars): Carrie Bow Cay (CB; N = 10), Curlew Cay (C; N = 5), and Southwater Cay (SW; N = 5), and Grand Cayman (dark bars): Kittiwake Anchor Chain (KA; N = 10), Sentinel (S; N = 4), and Slaughterhouse Wall (WS; N = 5). Bars with different lowercase letters are significantly different ($p < 0.05$) by Tukey's post hoc tests. Numbers in the upper right of each panel represent specific compounds; refer to Fig. 1 for compound names and structures. Note the different scales in each panel, and that compounds 5 and 11 are not included since they did not exhibit significant changes across sites

oroidin content was actually lower than that of purified oroidin (EC_{25} = 0.13 v. 0.48 mg ml^{-1}; Fig. 7), suggesting that the extract contained additional antibacterial metabolite(s) acting in concert with oroidin. Importantly, this extract also had the highest relative concentration of peak 10 (4,5-dibromo-1H-pyrrole-2-carboxylic acid; peak area = 1 197 583), relative to its concentrations in the extracts with intermediate and low amounts of oroidin (peak area = 331 034 and 63 649, respectively). This is also consistent with the multiple regression model, which predicted that 4,5-dibromo-1H-pyrrole-2-carboxylic acid was correlated with antibacterial activity against *S. marcescens*, albeit with a lower effect size (f^2 = 0.2) than oroidin (Table 2).

4. DISCUSSION

4.1. Site- and depth-specific variability in *Agelas tubulata* secondary metabolites

A. tubulata exhibits variability in the production of several secondary metabolites between sites in Belize and Grand Cayman; however, there were no signifi-

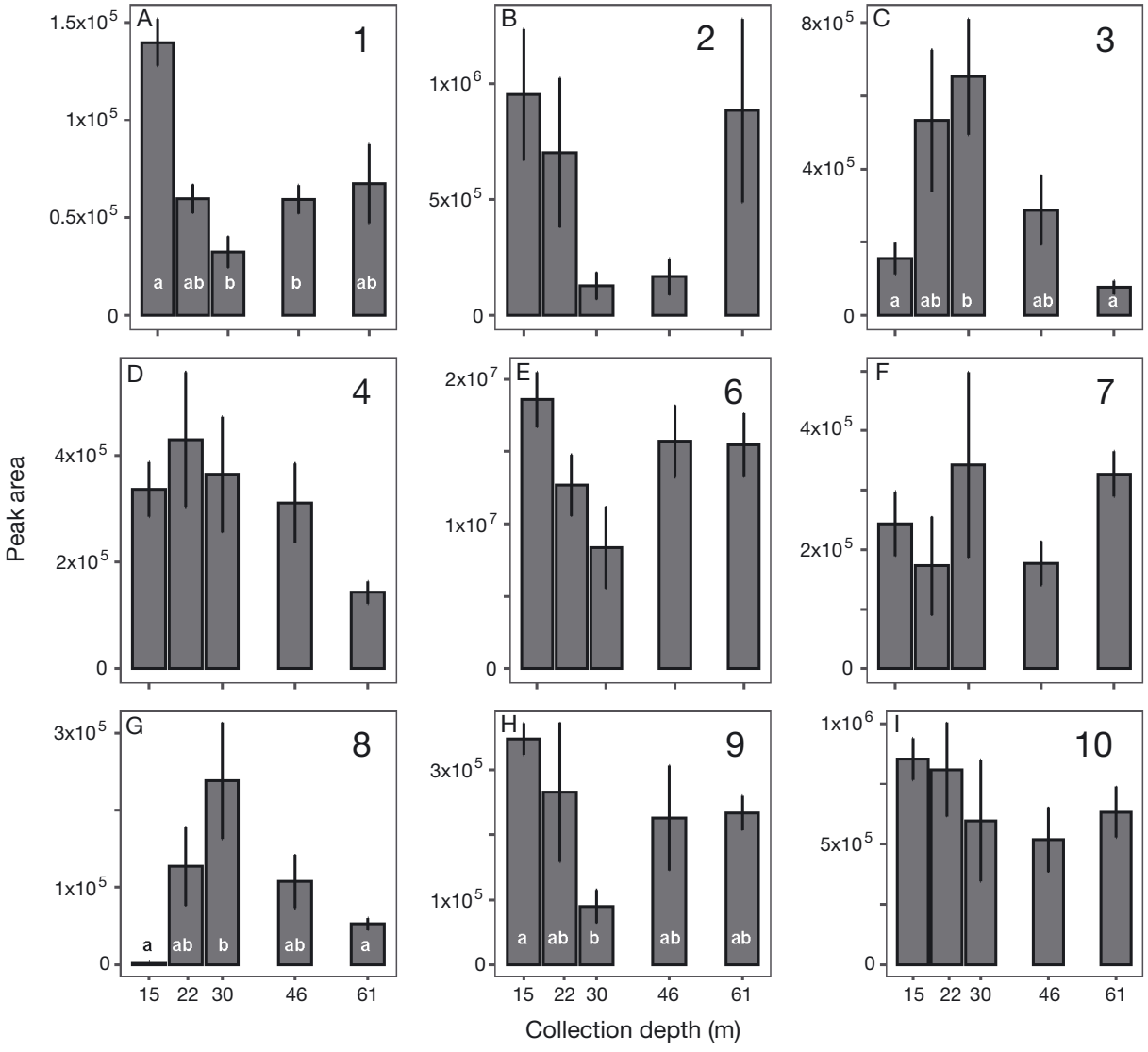

Fig. 3. Relative abundance of individual compounds within *Agelas tubulata* extracts by collection depth. Bars represent the mean (±SE) peak area of individual compounds within extracts from sponges collected from depths of 15–61 m in Grand Cayman. Sample sizes varied by depth, with N = 19 replicates at 15 m, and 5 replicates each at 22, 30, 46, and 61 m. Bars with different lowercase letters are significantly different ($p < 0.05$) by Tukey's post hoc tests. Numbers in the upper right of each panel represent specific compounds; refer to Fig. 1 for compound names and structures. Note the different scales in each panel, and that compounds 5 and 11 are not included since they did not exhibit significant changes across depths

cant differences in total extract concentration between sponges from the same depth (15 m) across sites. This disparity between variation in relative concentrations of constituent metabolites and the total extract concentration suggests some degree of trade-off between the biosynthetic end products (Fig. S3). Variation in concentrations of specific compounds among sites may be due to differences in levels of constitutive defenses relative to ecological or environmental conditions (e.g. predation pressure: Slattery et al. 2001). However, Belize and Grand Cayman have comparable levels of sponge predation (Lesser & Slattery 2013, Loh & Pawlik 2014, D. Gochfeld unpubl. data), so spongivory likely does not account for the differences in defensive metabolites between sites. The concentrations of agelongine, debromooxysceptrin, and ageliferin were higher at sites within Belize compared to sites within Grand Cayman, which parallels differences in the proximate biochemical composition of these same sponges (Clayshulte Abraham et al. 2021). Carbohydrate content was higher in sponges from Belize, while lipid content was higher in sponges from Grand Cayman (Clayshulte Abraham et al. 2021). Since these sam-

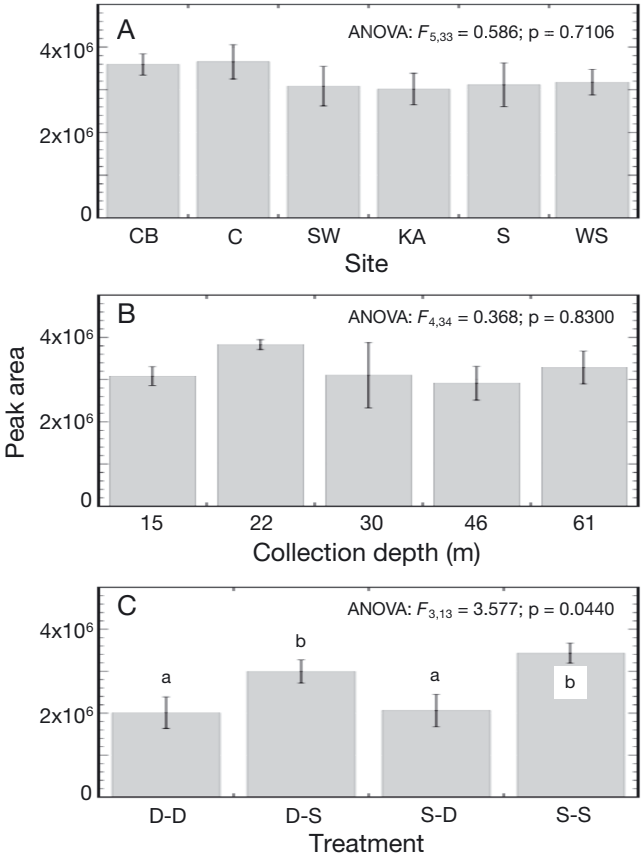

Fig. 4. Relative abundance of sceptrin within *Agelas tubulata* extracts by (A) collection site, (B) depth, and (C) transplant treatment. Bars represent the mean (±SE) peak area of the compound within extracts from sponges collected from 15 m at different sites in Belize and Grand Cayman (site abbreviations as in Fig. 2) at depths of 15–61 m in Grand Cayman, and from sponges transplanted from 22 m (shallow) to 61 m (deep) (S-D; N = 3), 61 to 22 m (D-S; N = 4), 22 to 22 m (S-S; N = 5), or 61 to 61 m (D-D; N = 5) in Grand Cayman. Bars with different lowercase letters are significantly different ($p < 0.05$) by Tukey's post hoc tests

ples were collected during the winter in Grand Cayman and the spring in Belize, these differences could be due to trade-offs with sponge reproductive status, which could also impact energy allocation to defensive metabolite production. Alternatively, seasonal variation in biotic and abiotic factors can affect defensive metabolite production (e.g. trophic subsidies: Page et al. 2005; microbiome: Anderson et al. 2010; temperature: Reverter et al. 2016). However, dissolved organic carbon accounts for 97.4% of carbon consumption by shallow-water *Agelas* spp. (Slattery & Lesser 2015), and these levels were essentially equivalent at our 2 sites during collections (Clayshulte Abraham et al. 2021, Macartney et al. 2021), so food resources were likely not the cause of differences in defensive metabolites.

The depth gradient in Grand Cayman represents a much narrower spatial scale (hundreds of meters) than between Belize and Grand Cayman (hundreds of kilometers), but the ecological differences between shallow and mesophotic reefs are much greater than those between shallow reefs (Lesser et al. 2018). Specifically, the light gradient is extreme enough to affect biosynthesis of sponge metabolites (Turon et al. 2009), and depth-specific differences in predation (Slattery et al. 2016), competition (Slattery & Lesser 2014, 2021), or sponge-associated microbial assemblages (Olson & Gao 2013) could also affect defensive metabolite production. Tissue extract concentrations in deep reef sponges (61 m) were 3 times higher than extract concentrations in shallow sponges (15 m). However, it is unlikely that the differences in extract concentrations were due to differential predation, since Macartney et al. (2021) reported no differences in bite scars on *A. tubulata* across the depth gradient. Instead, the increase in extract concentration could be a direct and/or indirect consequence of increased particulate organic matter (POM), a major source of sponge nutrition at depth (Lesser 2006, Lesser & Slattery 2013, Lesser et al. 2019, 2020, Macartney et al. 2021). If defensive metabolites are energetically costly to produce (e.g. Uriz et al. 1995, Machado et al. 2017), then the increased availability of POM resources with increasing depth may provide the energetic surplus to facilitate their production (Ferretti et al. 2009). It is also possible that greater competition for space at mesophotic depths (Slattery & Lesser 2014, 2021) might select for increased production of metabolites with allelopathic activities (Assmann et al. 2004, Slattery & Gochfeld 2012).

Several compounds were differentially produced across the depth gradient, including agelongine, dispacamide C, and bromosceptrin/bromoageliferin. Although these compounds are constituents of a putative shared biosynthetic pathway (Fig. S3, and see Rane et al. 2014), it is interesting that most of the compounds that varied across depths are different from those that varied between shallow reef sites. Mesophotic reef structure and function are very different than that of shallow coral reefs (Lesser et al. 2018), resulting in unique physiological adaptations (Lesser et al. 2010, 2019) that select for distinct biochemical phenotypes (Slattery et al. 2016, Slattery & Lesser 2021). Despite significant differences in sponge growth as a function of transplant treatment (Macartney et al. 2021), only 1 metabolite, sceptrin, varied between transplanted sponges and their back-transplanted controls. Sceptrin is a feeding deterrent against *Thalassoma bifasciatum* (Assmann et al.

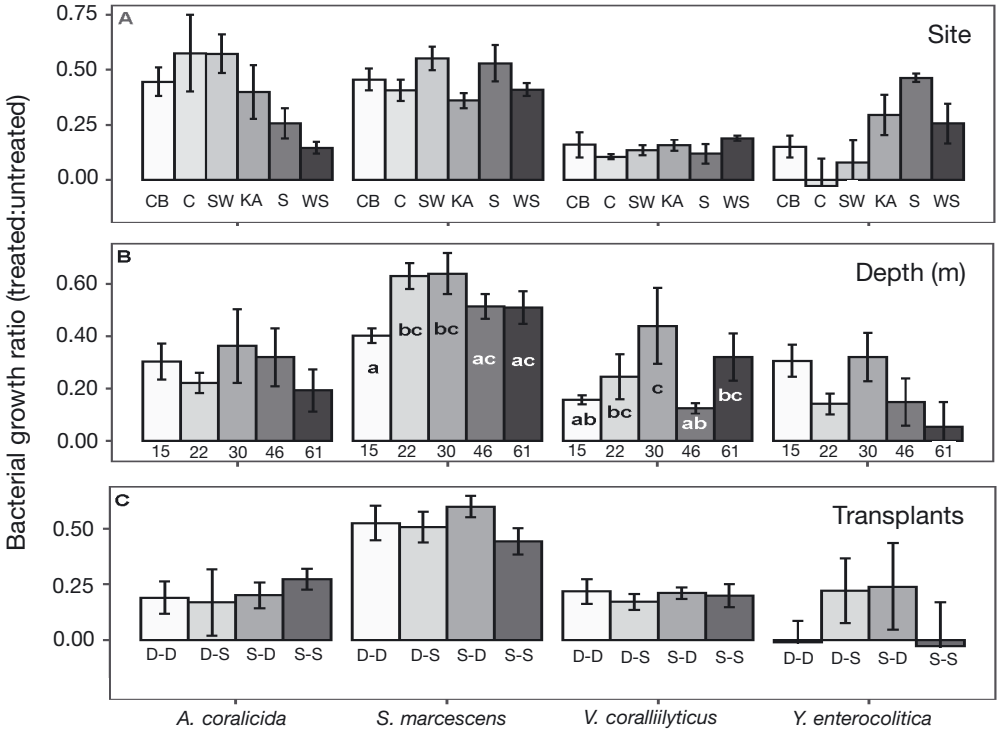

Fig. 5. Antibacterial activity of *Agelas tubulata* extracts by (A) collection site (at 15 m), (B) depth, and (C) transplant treatment. Site abbreviations as in Fig. 2; transplant treatments as in Fig. 4. Bars represent the mean (±SE) ratio of bacterial growth in treated (with sponge extracts) vs. untreated wells for each bacterial species: *Aurantimonas coralicida*, *Serratia marcescens*, *Vibrio coralliilyticus*, and *Yersinia enterocolitica*. N = 2–9 extracts per bar. Bars with different lowercase letters are significantly different ($p < 0.05$) by Tukey's post hoc tests within a bacterial species

Table 2. Summary of multiple regression models predicting antibacterial activity against 4 bacterial strains (*Aurantimonas coralicida*, *Serratia marcescens*, *Vibrio coralliilyticus*, and *Yersinia enterocolitica*), based on ratios of bacterial growth in treated vs. untreated wells and relative compound concentrations in terms of peak area within *Agelas tubulata* extracts. Slope coefficients (β), *t*-and p-values, and Cohen's f^2 effect sizes are presented for individual compounds included in models. Also included is the predicted directional effect of each compound, as either promoting or inhibiting growth, for individual bacterial strains. Statistics for complete linear models are also reported

Bacteria	Compound	β	*t*	p	f^2	Effect on growth
A. coralicida	Debromooxysceptrin	4.14×10^{-8}	4.04	0.0001	–	Positive
Full linear model: df = 1,72; $F = 16.3$; p = 0.0001; $R^2 = 0.17$; intercept = –0.756						
S. marcescens	Debromooxysceptrin	-1.69×10^{-8}	–5.27	<0.0001	0.65	Negative
	Oxysceptrin	-2.22×10^{-7}	–3.2	0.002	0.24	Negative
	Oroidin	-1.52×10^{-8}	–10.1	<0.0001	1.67	Negative
	4,5-Dibromo-1H-pyrrole-2-carboxylic acid	-8.01×10^{-8}	–2.38	0.02	0.2	Negative
	Dibromoageliferin	1.73×10^{-7}	4.16	0.0001	0.41	Positive
Full linear model: df = 5,368; $F = 11.5$; p < 0.0001; $R^2 = 0.40$; intercept = –0.287						
V. coralliilyticus	Agelongine	-4.43×10^{-7}	–4.03	<0.0002	0.39	Negative
	Oxysceptrin	-5.53×10^{-7}	–4.50	<0.0001	0.40	Negative
	4,5-Dibromo-1H-pyrrole-2-carboxylic acid	-7.61×10^{-7}	–1.51	0.14	0.15	Negative
	Dibromoageliferin	3.79×10^{-7}	5.42	<0.0001	0.46	Positive
Full linear model: df = 4,294; $F = 11.1$; p < 0.0001; $R^2 = 0.45$; intercept = –0.77						
Y. enterocolitica	Agelongine	-6.05×10^{-7}	–3	0.004	0.15	Negative
	Oxysceptrin	4.3×10^{-7}	–1.95	0.06	0.05	Positive
Full linear model: df = 2,146; $F = 5.57$; p = 0.006; $R^2 = 0.13$; intercept = –0.820						

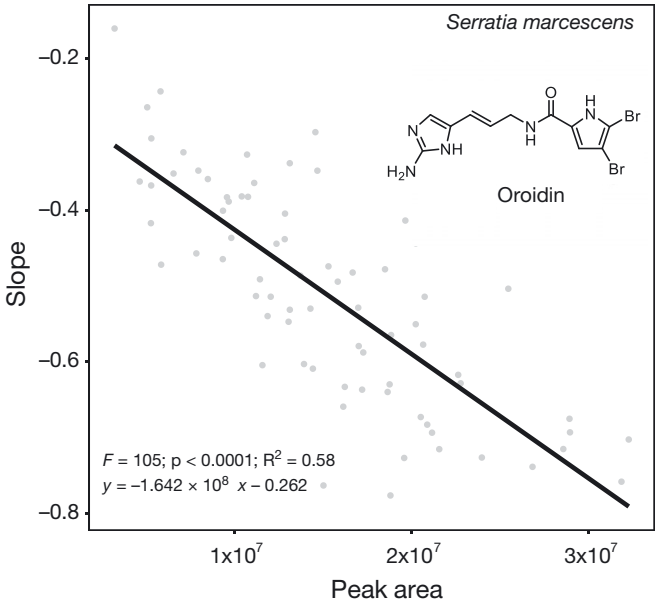

Fig. 6. Partial regression of the relative concentration (peak area) of oroidin and antibacterial activity (i.e. ratio of extract-treated vs. untreated wells) of *Agelas tubulata* extracts against *Serratia marcescens*, showing a positive relationship between relative concentration of oroidin within sponge extracts and antibacterial activity

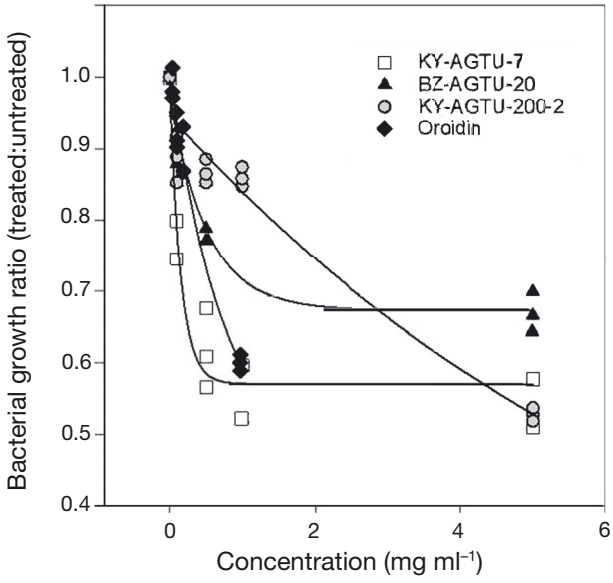

Fig. 7. Dose response curves for *Serratia marcescens* to purified oroidin (black diamonds; R^2 = 0.97, EC_{25} = 0.48 mg ml^{-1} [1.22 mM]) and representative *Agelas tubulata* extracts with a relatively high amount of oroidin (KY-AGTU-7; white squares: R^2 = 0.94, EC_{25} = 0.13 mg ml^{-1}), an intermediate amount of oroidin (BZ-AGTU-20; black triangles: R^2 = 0.89, EC_{25} = 0.71 mg ml^{-1}), and a relatively low amount of oroidin (KY-AGTU-200-2; grey circles: R^2 = 0.93, EC_{25} = 1.95 mg ml^{-1})

2000), *Stegastes partitus* (Richelle-Maurer et al. 2003), and *Canthigaster rostrata* (D. Gochfeld & M. Slattery unpubl. data), but not against *C. solandri* (Rohde et al. 2012), and it exhibits antimicrobial (Kelly et al. 2005) and allelopathic activity (Richelle-Maurer et al. 2003). Experimental wounding increased sceptrin production (Richelle-Maurer et al. 2003), but in the present study, this compound varied in concentration even in the absence of an apparent inductive cue (e.g. bite scars: Macartney et al. 2021), although we cannot rule out effects of microbial or allelopathic origin. It is possible that the growth tags we inserted into the sponges could have induced sceptrin production in the transplants, but the fact that tags were attached to all transplant sponges, and concentrations were comparable in transplants and back-transplants, suggests that any artifacts of this stress were likely ephemeral at best. Overall, the results of the transplant experiment indicate that phenotypic plasticity is rare in *A. tubulata*, and most metabolites are expressed at depth-specific constitutive levels.

Sponge-associated bacteria are assumed to play a role in the production of secondary metabolites, particularly those that are halogenated (Agarwal et al. 2014, Rua et al. 2018, but see Richelle-Maurer et al. 2003). Thus, the similar metabolite profiles among the transplanted sponges might suggest a lack of microbial variation within these transplants (e.g. Anderson et al. 2010). In fact, microbiomes did not vary among *A. tubulata* that occur naturally across the depth gradient (Macartney et al. 2022), yet metabolite profiles varied across these depths. Olson & Gao (2013) also found minimal variation in bacterial assemblages in *A. conifera* (now known to be *A. tubulata*: Pankey et al. 2022) in Little Cayman. These data are inconsistent with secondary metabolism being driven solely by changes in the composition of the *A. tubulata* microbiome.

4.2. Differences in antibacterial activity between populations of *A. tubulata*

The extracts from *A. tubulata* exhibited antibacterial activity against the panel of marine pathogens. These results were not surprising, since the *A. tubulata* extracts contained at least 8 bromopyrrole alkaloids, many of which are known to exhibit antimicrobial activity (Richelle-Maurer et al. 2003, Rane et al. 2014, Zhang et al. 2017). While there was some degree of species-specificity in antibacterial activity of the sponge extracts (i.e. greater activity against *Aurantimonas coralicida* and *Serratia marcescens*),

there was no difference in antibacterial activity relative to site. However, there were differences in antibacterial activity against both *S. marcescens* and *Vibrio coralliilyticus* across the shallow to mesophotic depth gradient, likely due to depth-specific selective pressures (Lesser et al. 2019). Transplanting sponges between depths, or back-transplanting them to their native depths, did not alter antimicrobial activity. In contrast, *Plakortis angulospiculatus* transplanted from mesophotic to shallow depths exhibited induced responses to increased spongivory on shallow reefs (Slattery et al. 2016). *A priori* we expected higher antibacterial activity at mesophotic depths (30–150 m) where bacterioplankton levels are highest (e.g. Macartney et al. 2021); however, antibacterial activity was highest at intermediate depths (22–30 m). This may be indicative of greater microbial diversity, and thus a greater chance of pathogen exposure, at transitional depths (= shallow to upper mesophotic reefs), where coral reef biodiversity is particularly high (Lesser et al. 2019).

The predicted activity of specific metabolites based on the multiple regression models supports sponge selectivity for or against certain bacteria. For example, both debromooxysceptrin and oroidin inhibited growth of *S. marcescens*, but debromooxysceptrin could promote growth of *A. coralicida.* The relative tissue concentration of debromooxysceptrin in sponges from Carrie Bow Cay in Belize was approximately 4 times higher than in sponges from Kittiwake Anchor Chain in Grand Cayman, while the concentration of oroidin in sponges collected from Carrie Bow Cay was about half that of sponges collected from Kittiwake Anchor Chain. Thus, site-specific ecological pressures likely favor specific bioactive metabolites within a biosynthetic product pool (Arndt & Riedrich 2008, Rane et al. 2014) that have overlapping, but also unique, ecological roles (i.e. broad spectrum vs. selective microbial control; Gochfeld et al. 2012). Sponges such as *A. tubulata* host complex symbiotic microbial assemblages (Gloeckner et al. 2014), and the ability to tailor selectivity against potential pathogens while promoting the growth of beneficial bacteria may be critical in regulating microbial populations of the constituent host (Ritchie 2006, Kvennefors et al. 2012, Raina et al. 2016). The production of a suite of metabolites via a common biosynthetic pathway may be one adaptation to fine-tune control over the composition of a sponge microbiome.

This study demonstrated intraspecific variation in the production of secondary metabolites in populations of *A. tubulata* across sites and depths, and phenotypic plasticity in the compound sceptrin when sponges were transplanted between depths. These data are consistent with the presence of an inducible defense system that is locally adapted to site- or depth-specific cues (Karban & Baldwin 1997), although the specific cues were not identified in this study. This chemical variability corresponds to differences in antibacterial activity, which can aid in selection against specific bacterial species relative to local ecological conditions. This chemical tailoring may help to explain the relative stability observed in the microbiome of *A. tubulata* across environmental gradients (Olson & Gao 2013, Macartney et al. 2022). Given a future where sponge density increases, resulting in reduced distances between individuals, the likelihood of increased sponge disease (sensu Slattery & Gochfeld 2012) may result in the biosynthesis of, and selection for, antibacterial compounds that have significant implications for disease resistance in sponges, and contributions to the resilience of coral reef communities in the Anthropocene.

Acknowledgements. We thank Melinda Ansley, Brittany Sims, Amelia Mellor, M. Ryan Cox, and M. Claire Vickers for assistance in the laboratory; Dr. Andia Chaves Fonnegra, Dr. M. Sabrina Pankey, Elizabeth Kintzing, and Ann Fairly Barnett for help with sample collection; and Dr. Jessica Pruett for reviewing the manuscript. Sponge samples were collected under Belize Marine Scientific Research Permit Number 000034-17 and a Cayman Islands Government Department of Environment Research Permit. Logistical support was provided by the Smithsonian Caribbean Coral Reef Ecosystems Program's Carrie Bow Cay Marine Field Station in Belize and the staff of InDepth Water Sports in Grand Cayman. This project was funded by National Science Foundation grants OCE-1632333 to M.S., OCE-1638289 to M.S. and D.J.G., OCE-1632348 and 1638296 to M.P.L., and a University of Mississippi Graduate Student Council Research Award to A.C.A.

LITERATURE CITED

Agarwal V, El Gamal AA, Yamanaka K, Poth D and others (2014) Biosynthesis of polybrominated aromatic organic compounds by marine bacteria. Nat Chem Biol 10: 640–647

Anderson SA, Northcote PT, Page MJ (2010) Spatial and temporal variability of the bacterial community in different chemotypes of the New Zealand marine sponge *Mycale hentscheli.* FEMS Microbiol Ecol 72:328–342

Arndt HD, Riedrich M (2008) Synthesis of marine alkaloids from the oroidin family. Angew Chem Int Ed 47: 4785–4788

Assmann M, Lichte E, Pawlik JR, Köck M (2000) Chemical defenses of the Caribbean sponges *Agelas wiedenmayeri* and *Agelas conifera.* Mar Ecol Prog Ser 207:255–262

Assmann M, Lichte E, Köck M (2004) Multiple defensive roles for bromopyrrole alkaloids from Caribbean *Agelas* sponges. Boll Mus Ist Biol Univ Genova 68:187–193

Bayona LM, van Leeuwen G, Erol O, Swierts T, van der Ent E, de Voogd NJ, Choi YH (2020) Influence of geographical location on the metabolic production of giant barrel sponges (*Xestospongia* spp.) revealed by metabolomics tools. ACS Omega 5:12398–12408

Bell JJ, Davy SK, Jones T, Taylor MW, Webster NS (2013) Could some coral reefs become sponge reefs as our climate changes? Glob Change Biol 19:2613–2624

Ben-Haim Y, Thompson FL, Thompson CC, Cnockaert MC, Hoste B, Swings J, Rosenberg E (2003) *Vibrio coralliilyticus* sp. nov., a temperature-dependent pathogen of the coral *Pocillopora damicornis*. Int J Syst Evol Microbiol 53:309–315

Chanas B, Pawlik JR, Lindel T, Fenical W (1997) Chemical defense of the Caribbean sponge *Agelas clathrodes* (Schmidt). J Exp Mar Biol Ecol 208:185–196

Clayshulte Abraham A, Gochfeld D, Macartney K, Mellor A, Lesser M, Slattery M (2021) Biochemical variability in sponges across the Caribbean basin. Invertebr Biol 140: e12341

Cronin G (2001) Resource allocation in seaweeds and marine invertebrates: chemical defense patterns in relation to defence theories. In: McClintock JB, Baker BJ (eds) Marine chemical ecology. CRC Press, Boca Raton, FL, p 325–353

de Brito RC, da Silva GN, Farias TC, Ferreira PB, Ferreira SB (2017) Standardization of the safety level of the use of DMSO in viability assays in bacterial cells. In: Proc MOL2NET 2017 Conf on Molecular, Biomedical & Computational Sciences and Engineering, January 15, 2017, 3rd edn. MDPI, Basel

Deignan LK, Pawlik JR (2016) Demographics of the Caribbean brown tube sponge *Agelas tubulata* on Conch Reef, Florida Keys, and a description of *Agelas* Wasting Syndrome (AWS). Proc 13th Intl Coral Reef Symp, Honolulu, HI, p 72–84

Deignan LK, Pawlik JR, Erwin PM (2018) *Agelas* wasting syndrome alters prokaryotic symbiont communities of the Caribbean brown tube sponge, *Agelas tubulata*. Microb Ecol 76:459–466

Denner EBM, Smith GW, Busse HJ, Schulmann P and others (2003) *Aurantimonas coralicida* gen. nov., sp. nov., the causative agent of white plague type II on Caribbean scleractinian corals. Int J Syst Evol Microbiol 53: 1115–1122

Easson CG, Slattery M, Momm HG, Olson JB, Thacker RW, Gochfeld DJ (2013) Exploring individual- to population-level impacts of disease on coral reef sponges: using spatial analysis to assess the fate, dynamics, and transmission of *Aplysina* red band syndrome (ARBS). PLOS ONE 8:e79976

Ferretti C, Vacca S, de Ciucis C, Marengo B and others (2009) Growth dynamics and bioactivity variation of the Mediterranean demosponges *Agelas oroides* (Agelasida, Agelasidae) and *Petrosia ficiformis* (Haplosclerida, Petrosiidae). Mar Ecol 30:327–336

Gloeckner V, Wehrl M, Moitinho-Silva L, Gernert C and others (2014) The HMA-LMA dichotomy revisited: an electron microscopical survey of 56 sponge species. Biol Bull (Woods Hole) 227:78–88

Gochfeld DJ, Aeby GS (2008) Antibacterial chemical defenses in Hawaiian corals provide possible protection from disease. Mar Ecol Prog Ser 362:119–128

Gochfeld DJ, Kamel HN, Olson JB, Thacker RW (2012) Trade-offs in defensive metabolite production but not ecological function in healthy and diseased sponges. J Chem Ecol 38:451–462

Han BN, Hong LL, Gu BB, Sun YT, Wang J, Liu JT, Lin HW (2019) Natural products from sponges. In: Li Z (ed) Symbiotic microbiomes of coral reefs sponges and corals. Springer, Dordrecht, p 329–463

Karban R, Baldwin IT (1997) Induced responses to herbivory. University of Chicago Press, Chicago, IL

Kelly SR, Garo E, Jensen PR, Fenical W, Pawlik JR (2005) Effects of Caribbean sponge secondary metabolites on bacterial surface colonization. Aquat Microb Ecol 40: 191–203

Kilinc B, Besler A (2014) The occurrence of enteric bacteria in marine environment and pollution. Mar Sci Tech Bull 3:39–43

Kozak M, Piepho H (2018) What's normal anyway? Residual plots are more telling than significance tests when checking ANOVA assumptions. J Agron Crop Sci 204: 86–98

Kvennefors EC, Sampayo E, Kerr C, Vieira G, Roff G, Barnes AC (2012) Regulation of bacterial communities through antimicrobial activity by the coral holobiont. Microb Ecol 63:605–618

Lesser MP (2006) Benthic–pelagic coupling on coral reefs: feeding and growth of Caribbean sponges. J Exp Mar Biol Ecol 328:277–288

Lesser MP, Slattery M (2013) Ecology of Caribbean sponges: Are top-down or bottom-up processes more important? PLOS ONE 8:e79799

Lesser MP, Slattery M, Stat M, Ojimi M, Gates RD, Grottoli A (2010) Photoacclimatization by the coral *Montastraea cavernosa* in the mesophotic zone: light, food, and genetics. Ecology 91:990–1003

Lesser MP, Slattery M, Mobley CD (2018) Biodiversity and functional ecology of mesophotic coral reefs. Annu Rev Ecol Evol Syst 49:49–71

Lesser MP, Slattery M, Laverick JH, Macartney KJ, Bridge TC (2019) Global community breaks at 60 m on mesophotic coral reefs. Glob Ecol Biogeogr 28:1403–1416

Lesser MP, Mueller B, Pankey MS, Macartney KJ, Slattery M, de Goeij JM (2020) Depth-dependent detritus production in the sponge, *Halisarca caerulea*. Limnol Oceanogr 65:1200–1214

Loh TL, Pawlik JR (2014) Chemical defenses and resource trade-offs structure sponge communities on Caribbean coral reefs. Proc Natl Acad Sci USA 111:4151–4156

Macartney K, Clayshulte Abraham A, Slattery M, Lesser M (2021) Growth and feeding in the sponge, *Agelas tubulata*, from shallow to mesophotic depths on Grand Cayman. Ecosphere 12:e03764

Macartney KJ, Pankey MS, Clayshulte Abraham A, Slattery M, Lesser MP (2022) Depth dependent trophic strategies of Caribbean sponges on mesophotic coral reefs. Mar Ecol Prog Ser (in press), https://doi.org/10.3354/meps14059

Machado RA, Zhou W, Ferrieri AP, Arce CCM, Baldwin IT, Xu S, Erb M (2017) Species-specific regulation of herbivory-induced defoliation tolerance is associated with jasmonate inducibility. Ecol Evol 7:3703–3712

Newbold RW, Jensen PR, Fenical W, Pawlik JR (1999) Antimicrobial activity of Caribbean sponge extracts. Aquat Microb Ecol 19:279–284

Oksanen J, Blanchet FG, Friendly M, Kindt R and others (2020) Vegan: community ecology package, R version 2.5-7. https://github.com/vegandevs/vegan

Olson JB, Gao Z (2013) Characterizing the bacterial associates of three Caribbean sponges along a gradient from shallow to mesophotic depths. FEMS Microbiol Ecol 85: 74–84

Page M, West L, Northcote P, Battershill C, Kelly M (2005) Spatial and temporal variability of cytotoxic metabolites in populations of the New Zealand sponge *Mycale hentscheli.* J Chem Ecol 31:1161–1174

Pankey MS, Plachetzki DC, Macartney KJ, Gastaldi M, Slattery M, Gochfeld DJ, Lesser MP (2022) Cophylogeny and convergence shape holobiont evolution in sponge-microbe symbioses. Nat Ecol Evol doi:10.1038/s41559-022-01712-3

Patterson KL, Porter JW, Ritchie KB, Polson SW and others (2002) The etiology of white pox, a lethal disease of the Caribbean elkhorn coral, *Acropora palmata.* Proc Natl Acad Sci USA 99:8725–8730

Pavia H, Toth GB (2000) Inducible chemical resistance to herbivory in the brown seaweed *Ascophyllum nodosum.* Ecology 81:3212–3225

Pawlik JR (2011) The chemical ecology of sponges on Caribbean reefs: natural products shape natural systems. Bioscience 61:888–898

Pawlik JR (2012) Antipredatory defensive roles of natural products from marine invertebrates. In: Fattorusso E, Gerwick WH, Taglialatela-Scafati O (eds) Handbook of marine natural products. Springer, New York, NY, p 677–710

Qian PY, Xu SY (2012) Antifouling activity of marine natural products. In: Fattorusso E, Gerwick WH, Taglialatela-Scafati O (eds) Handbook of marine natural products. Springer, New York, NY, p 749–821

R Core Team (2020) R: a language and environment for statistical computing. R Foundation for Statistical Computing, Vienna. www.R- project.org

Raina JB, Tapiolas D, Motti CA, Foret S and others (2016) Isolation of an antimicrobial compound produced by bacteria associated with reef-building corals. PeerJ 4:e2275

Rane R, Sahu N, Shah C, Karpoormath R (2014) Marine bromopyrrole alkaloids: synthesis and diverse medicinal applications. Curr Top Med Chem 14:253–273

Reverter M, Perez T, Ereskovsky AV, Banaigs B (2016) Secondary metabolome variability and inducible chemical defenses in the Mediterranean sponge *Aplysina cavernicola.* J Chem Ecol 42:60–70

Reverter M, Tribalat MA, Pérez T, Thomas OP (2018) Metabolome variability for two Mediterranean sponge species of the genus *Haliclona*: specificity, time, and space. Metabolomics 14:114

Richelle-Maurer E, DeKluijver MJ, Feio S, Guadêncio S and others (2003) Localization and ecological significance of oroidin and sceptrin in the Caribbean sponge *Agelas conifera.* Biochem Syst Ecol 31:1073–1091

Ritchie KB (2006) Regulation of microbial populations by coral surface mucus and mucus-associated bacteria. Mar Ecol Prog Ser 322:1–14

Rohde S, Gochfeld DJ, Ankisetty S, Avula B, Schupp PJ, Slattery M (2012) Spatial variability in secondary metabolites of the Indo-Pacific sponge *Stylissa massa.* J Chem Ecol 38:463–475

Rua CPJ, de Oliveira LS, Froes A, Tschoeke DA and others (2018) Microbial and functional biodiversity patterns in sponges that accumulate bromopyrrole alkaloids suggest horizontal gene transfer of halogenase genes. Microb Ecol 76:825–838

Sacristán-Soriano O, Banaigs B, Becerro MA (2011) Relevant spatial scales of chemical variation in *Aplysina aerophoba.* Mar Drugs 9:2499–2513

Slattery M, Gochfeld DJ (2012) Chemically mediated competition and host–pathogen interactions among marine organisms. In: Fattorusso E, Gerwick WH, Taglialatela-Scafati O (eds) Handbook of marine natural products. Springer, New York, NY, p 823–859

Slattery M, Lesser MP (2014) Allelopathy in the tropical alga *Lobophora variegata* (Phaeophyceae): mechanistic basis for a phase shift on mesophotic coral reefs? J Phycol 50: 493–505

Slattery M, Lesser MP (2015) Trophic ecology of sponges from shallow to mesophotic depths (30 to 150 m): Comment on Pawlik et al. (2015). Mar Ecol Prog Ser 527:275–279

Slattery M, Lesser MP (2021) Gorgonians are foundation species on sponge-dominated mesophotic coral reefs in the Caribbean. Front Mar Sci 8:654268

Slattery M, Starmer J, Paul V (2001) Temporal and spatial variation in defensive metabolites of the tropical Pacific soft corals *Sinularia maxima* and *S. polydactyla.* Mar Biol 138:1183–1193

Slattery M, Gochfeld DJ, Diaz MC, Thacker RW, Lesser MP (2016) Variability in chemical defense across a shallow to mesophotic depth gradient in the Caribbean sponge *Plakortis angulospiculatus.* Coral Reefs 35:11–22

Strauss J, Reyes-Dominguez Y (2011) Regulation of secondary metabolism by chromatin structure and epigenetic codes. Fungal Genet Biol 48:62–69

Taylor MW, Radax R, Steger D, Wagner M (2007) Sponge-associated microorganisms: evolution, ecology, and biotechnological potential. Microbiol Mol Biol Rev 71: 295–347

Thompson J, Murphy P, Berquist P, Evans E (1987) Environmentally induced variation in diterpene composition of the marine sponge *Rhopaloeides odorabile.* Biochem Syst Ecol 15:595–606

Turon X, Martí R, Uriz MJ (2009) Chemical bioactivity of sponges along an environmental gradient in a Mediterranean cave. Sci Mar 73:387–397

Uriz MJ, Turon X, Becerro MA, Galera J, Lozano J (1995) Patterns of resource allocation to somatic, defensive, and reproductive functions in the Mediterranean encrusting sponge *Crambe crambe* (Demospongiae, Poecilosclerida). Mar Ecol Prog Ser 124:159–170

Van Soest RWM, Boury-Esnault N, Vacelet J, Dohrmann M and others (2012) Global diversity of sponges (Porifera). PLOS ONE 7:e35105

Wang J, Liu H, Zhao J, Gao H and others (2010) Antimicrobial and antioxidant activities of the root bark essential oil of *Periploca sepia* and its main component 2-hydroxy-4-methoxybenzaldehyde. Molecules 15:5807–5817

Wulff JL (2021) Targeted predator defenses of sponges shape community organization and tropical marine ecosystem function. Ecol Monogr 91:e01438

Zhang H, Dong M, Chen J, Wang H, Tenney K, Crews P (2017) Bioactive secondary metabolites from the marine sponge *Agelas.* Mar Drugs 15:351

Editorial responsibility: Paul Snelgrove, St. John's, Newfoundland and Labrador, Canada
Reviewed by: 2 anonymous referees

Submitted: September 24, 2021
Accepted: March 21, 2022
Proofs received from author(s): May 13, 2022